Memoirs of the Faculty of Engineering, Kyushu University, Vol.73, No.1, June 2013

Proposed Analysis on Output Currents of Electrochemical Apparatus with Regards to Weak Interaction

by

Nur AIDA[*], Kenji ISHIBASHI[**], Youichi IMAHAYASHI[*],
Shoya SUDA[*] and Shouhei NAKAMURA[*]

(Received May 7, 2013)

Abstract

We analyze the interaction of antineutrinos with water particles in electrochemical apparatuses. The analysis is based on the postulation that low-energy neutrinos readily interact with water molecules under a scalar auxiliary field, and the reaction products assist electrochemical reactions to generate output current. We formulate the output current of neutrino interaction in the electrochemical apparatus with an electrochemical half-cell model under the postulated influence of weak interaction. Experiments of two types are considered; they are reactions by either environmental neutrinos or nuclear-reactor-neutrino irradiation. The output currents are treated to be generated by hydrogen ions and oxygen gas with an electrochemical half-cell model. The same electrochemical parameters are applied to analysis, and it leads to successful reproduction of experimental data. The agreement suggests that there may be electrochemical reactions that are assisted by weak interaction.

Keywords: Electrochemical detector, Raw silk, Neutrino, Scalar auxiliary field, Half-cell model

1. Introduction

Neutrinos make only the weak interaction. The interaction cross sections are as small as 10^{-41} to 10^{-38} cm^2 for neutrinos with energies around 1MeV [1)]. In a low-energy region, solar neutrinos were measured by radiochemical experiments such as SAGE[2)], where the neutrino detection threshold was 0.23 MeV. Neutrinos with energies below this energy have not been measured for far. It is known well in electrodynamics that the determination of electromagnetic potentials requires constraint conditions like Landau and Fermi gauges[3)]. Such gauges accompany a special auxiliary field[4),5)] (B^0 thereafter), except the Landau gauge giving the Lorentz condition for four-dimensional potential A^μ. The auxiliary field B^0 possesses an energy density like electric and magnetic fields.

* Graduate Student, Department of Applied Quantum Physics and Nuclear Engineering
** Professor, Department of Applied Quantum Physics and Nuclear Engineering

When considerably low energy neutrinos receive certain strength of external field such as auxiliary field B^0, it may disturb the mass-generation mechanism of neutrino. Although the mechanism is not elucidated completely, the external auxiliary field may give rise to influence to the mass state[6]. We may have found[7] the material that possibly generates the external field and promotes the weak-interaction reaction[7]. An electrochemical apparatus[7] was developed with the material for detecting low energy neutrinos. Experimental current signals were obtained for irradiation of both environmental and nuclear-reactor neutrinos. A signal generation scenario was proposed in the previous report[8], and quantitative calculations were not carried out yet. In this paper, we present quantitative analysis by introducing an electrochemical half-cell model under the influence of weak interaction.

2. Experiment

The electrochemical experiments were carried out by our group (Liu et al.[7]). The method is described briefly. **Figure 1** illustrates the experimental apparatus. The experimental apparatus was set in a Teflon container of 90 mm in length and 58 mm in diameter. Purified water of 50-g was poured in its lower half region. Gold and glassy carbon plates were used as the anode and cathode electrodes, respectively. They were both 20 mm x 50 mm in area. The thickness was 0.1 mm for the gold electrode and 1.0 mm for the carbon one. Electrodes were boiled in nitric acid for cleaning the surface. The electrodes were rinsed thoroughly in purified water by an ultrasonic washer. Purified water was bubbled by nitrogen gas before pouring the apparatus. The electrodes were placed in separation of 1 cm. Raw silk of 0.5-g in weight, chosen from biological material, was set on each side of gold electrode. The two electrodes were connected by copper wires to a voltmeter, where the input impedance was adjusted to be 1 MΩ with resistors. The value 1 MΩ was chosen from test experiments with input impedances of 0.3 to 4.5 MΩ. When the impedance was set, for example, at 0.3 MΩ, the voltage decreased to almost half value, but the product of voltage and current, i.e. power, was kept the same as in the case of 1 MΩ. The output signal is expressed by the current in this study. The experimental apparatus was placed in an incubator to be operated at a temperature of 27^0C (300K).

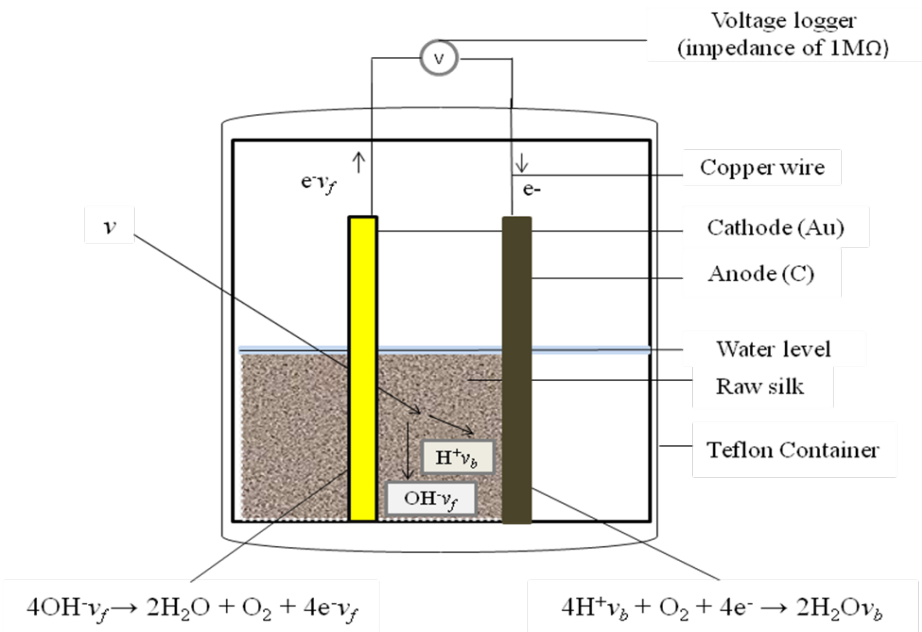

Fig.1 Experimental apparatus with explanation of proposed charge transfer process.

Experimental data[7] of two types will be analyzed in this paper; the first is the measurement in a laboratory of Kyushu university (Hakozaki campus) under natural environmental circumstances, and the second is the experiment performed under nuclear-reactor-neutrino irradiation. The environmental measurement was carried out with three apparatuses, and the experimental data by Liu et al.[7] are plotted by three kinds of marks in the lower part of **Fig. 2**. The variation in three measurements was 3% in one sigma. The initial peaks appear at 1.5 days. After the initial peak, the current signals fallen to almost zero values, then gradually increased, and subsequently reaches about 50 nA after 20 days. When the experiment was made without raw silk, the current fallen to zero within a day. In the case of use of other artificial fibers, the current also went to zero completely in few to several days[7].

The reactor-neutrino irradiation was carried out at the site of nuclear thermal reactor (electric power of 165 MW). The irradiation was made for three days at a distance of 35 m from the center of the reactor core. The antielectron neutrino flux was estimated to be 6 x 10^{11} $cm^{-2}s^{-1}$. The radiation dose in the experimental room of the irradiation was twice larger than natural radiation dose, that is, the experimental room was well shielded from neutrons and gamma rays. After irradiation, the apparatus was transported to the laboratory of Kyushu University. The experiment was continued there. The results[7] are shown by circles in the upper part of the figure. It is noted that the lower and the upper experiments were initiated simultaneously at the same time. The output current attained 90 nA in a day. It then decreased during the transportation and later time, but began to increase again after a week.

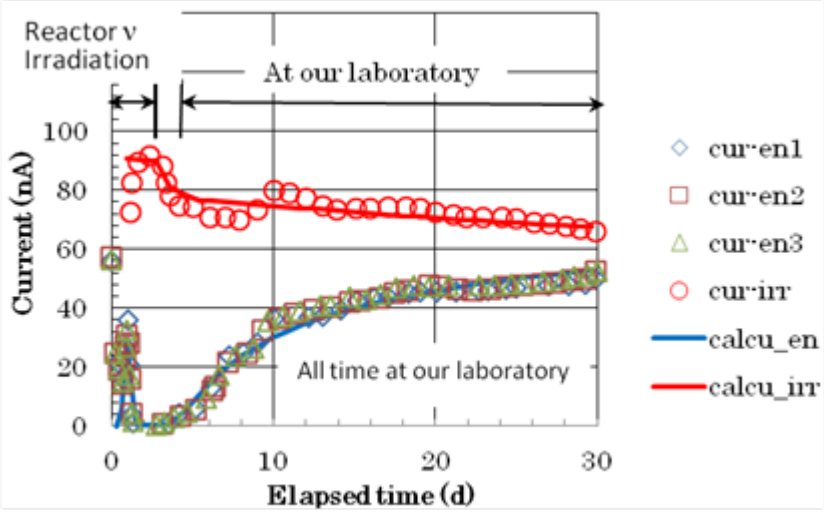

Fig. 2 Output current of the apparatus. The lower marks of three types are the results for the experiments performed under environmental conditions in a laboratory at Kyushu University, while the upper marks show the results obtained under reactor-neutrino irradiation and subsequent environmental conditions[7]. The solid curves indicate calculation results.

It is natural to consider that the larger currents in the upper data are ascribed to reactor antineutrinos. This suggests that the current in the lower data may also be caused by natural antineutrinos. We are concerned with the low energy antielectron neutrinos, which may have a size of internal structure comparable to atomic diameter. The antielectron neutrinos, for example, below 50 keV, have a fraction[9] of 8.0 x 10^{-3} to the total reactor neutrino flux. The natural radiations contain antielectron neutrinos, i.e. geoneutrinos. The geoneutrinos are generated in the interior of the

Earth mainly from the progenies of $^{238;235}$U, ^{232}Th and ^{40}K decays. The flux of geoneutrinos below 50 keV, for instance, was calculated by KAMLAND group and found to be 5.7 x 10^5 $cm^{-2}s^{-1}$ under the assumption of typical global abundances[10]. The ratio of the low-energy antielectron neutrino flux in the upper to that in the lower ones during the first three days is evaluated to be 9.5 x 10^3. We are interested in whether the two responses are quantitatively understood with basically the same procedure or not.

3. Chemical reactions

The electrode materials in the experimental apparatus are stable against most chemical reactions. In previous experiments[8),11)], (1) ICP mass measurements indicates that the density of solved ions from raw silk saturated within a few days, and (2) the direct measurement of oxygen gas showed that the output current increased with oxygen gas concentration. In the upper part of **Fig. 2**, the current glows quite immediately after being set near the nuclear reactor. This is not understood by the reduction and oxidation by oxygen gas at all. In the lower part of the same figure, the signal gradually increases within a few weeks. This behavior disagrees with the above experimental indication (1). The carbon material is often utilized as a reduction electrode for phosphoric-acid fuel cells[13)], and works for the electrochemical reaction of $4H^+ + O_2 + 4e \rightarrow 2H_2O$. The result (2) suggests the promotion of this kind of reaction in the apparatus.

For these reasons, we follow the signal generation scenario that was previously proposed[8)] by our group. The process is simply illustrated in **Fig. 1**. When a water molecule is dissociatively ionized into hydrogen ion (H^+) and hydroxide ions (OH^-), the threshold energy for the reaction is 0.84 eV. It was presumed that the raw silk produces scalar auxiliary field B[06)]. A neutrino is postulated[6)] to be composed of boson and fermion particles as $\nu_b\nu_f$. When the field energy of B^0 ascribed to the raw silk is large, it may increase the neutrino mass and make the neutrino unstable[6)]. The signal generation scenario is as follows [8)]. The neutrino may make a water molecule to break into hydrogen and hydroxide ions as

$$\nu_b\nu_f + H_2O \rightarrow H^+\nu_b + OH^-\nu_f . \qquad (1)$$

The repulsive properties[6)] of ν_b and ν_f at rest do not allow $H^+\nu_b$ and $OH^-\nu_f$ to be recombined. The hydroxide ions with fermion ($OH^-\nu_f$) may diffuse to the gold plate, and produce water molecules and oxygen gas with transferring $e^-\nu_f$ pairs to the electrode as

$$4OH^-\nu_f \rightarrow 2H_2O + O_2 + 4e^-\nu_f . \qquad \text{(Gold electrode)} \qquad (2)$$

The hydrogen ions with boson ($H^+\nu_b$) in Eq. (1) may move to the carbon plate. The oxygen gas generated in Eq. (2) may also arrive at this electrode, where $H^+\nu_b$ and O_2 receive the charge e that conducted through the connecting wire. The reduction reaction on the carbon electrode is given as

$$4H^+\nu_b + O_2 + 4e^- \rightarrow 2(H^+\nu_b)_2O. \qquad \text{(Carbon electrode)} \qquad (3)$$

This reaction is considered to keep the bound state between hydrogen and boson. Thus, the hydrogen and hydroxide ions in Eq. (1) were understood to produce water molecules, causing the charge transfer between electrodes. Similarly to the case of conventional OH^- and H^+ ions, Eqs.

(2) and (3) are considered to be endothermic and exothermic reactions, respectively. We postulate that the reaction of Eq. (2) is promoted by some catalyst effect related to the weak interaction by B^0. When this works, diffusions of ions and gas related to Eqs, (2) and (3) are expected to take place to produce the current through the conduction wire. Numerical computation will be performed with an analysis model.

4. Half-cell model

On the basis of the process in Eqs. (1-3), we attempt to describe the time evaluation of the output currents in **Fig. 2**. The usual formulation of electrochemical reaction in a standard text book[11] is adopted as a half-cell model, but the effect of the weak interaction is considered. For a reversible reaction on the carbon electrode, the current density j is written by using the reduction reaction rate v_c and the oxidation one v_a as

$$j = nF(v_c - v_a) = j_{\mathrm{H}^+} + j_{\mathrm{H_2O}}, \tag{4}$$

where n is the number of moving electrons in the reaction and F stands for the Faraday constant $F = eN_A$ with e the electron charge and N_A the Avogadro number. The reduction reaction rate is expressed by

$$v_c = P_c[\mathrm{H}^+ v_b]^4[\mathrm{O}_2]\exp\left(-\Delta G^{\neq}/RT\right), \tag{5}$$

where P_c stands for the reaction rate coefficient, R the gas constant, T the temperature and $\Delta G^{\neq}$ the free energy of activation. The bracket [ ] indicates concentration thereafter. The value of $\Delta G^{\neq}$ takes the form of

$$\Delta G^{\neq} = \Delta G^{0\neq} + \alpha nFE, \tag{6}$$

where $\Delta G^{0\neq}$ is the activation energy at zero bias voltage, E the bias voltage and α the transfer coefficient. Therefore, the current density j_{H^+} is given by the Butler-Volmer equation[11] as

$$j_{\mathrm{H}^+} = nFP_c[\mathrm{H}^+ v_b]^4[\mathrm{O}_2]\exp\left(-\frac{\Delta G^{0\neq} + \alpha nFE}{RT}\right). \tag{7}$$

Here, we set at $n = 4$ according to Eq. (3). Since the current is written as $I_{\mathrm{H}^+} = j_{\mathrm{H}^+}A$ with area A, the use of $\Delta G^{0\neq} = N_A\Delta$ in Eq. (7) leads to

$$I_{\mathrm{H}^+} = 4FAP_c[\mathrm{H}^+ v_b]^4[\mathrm{O}_2]\exp\left(-\frac{\Delta + 4\alpha eE}{k_BT}\right), \tag{8}$$

where k_B is the Boltzmann constant, and e the electron charge. Similarly, the density of water molecule may produce another current by the reverse reaction as

$$I_{\mathrm{H_2O}} = -4FAP_a[\mathrm{H_2O}]^2 \exp\left(-\frac{\Delta - 4(1-\alpha)eE}{k_B T}\right). \quad (9)$$

The oxidation electrode in Eq. (2) gives rise to the endothermic reaction (Q= – 0.40 eV). Therefore, the reaction in Eq. (2) is incapable of inducing the oxidation reaction without assistance such as catalyst. When the raw silk is present around the gold electrode, the energy difference of B^0 field between the regions inside and outside the gold plate may supply an energy compensating the exothermic reaction. In this case, Eq. (4) on the carbon electrode is supposed to determining the current as the half-cell model.

As an additional reaction, positive ions of Ca^{2+} and Na^{2+} were present[7] in the solution. Such ions were solved out from the raw silk into water. An impurity current I_{imp} is treated to be produced by a simple reduction reaction, and be formulated as

$$I_{\mathrm{imp}} = 4FAP_i[\mathrm{M}^{2+}]^2[\mathrm{O_2}]\exp\left(-\frac{\Delta + 4\alpha eE}{k_B T}\right). \quad (10)$$

The value of Δ is set at the same value in Eq. (6), but is actually corrected by the coefficient P_i with adjustable feature. The reverse current for I_{imp} is neglected in this study. Thus, the induced current becomes $I = I_{\mathrm{H^+}} + I_{\mathrm{H_2O}} + I_{\mathrm{imp}}$ with regard to the carbon electrode with the half-cell model.

5. Output current analysis by half-cell model

We analyze the experimental results in **Fig. 2** by using the half-cell model. The concentration $[\mathrm{OH^-}\, v_f\,]$ is implicitly taken to be the same as $[\mathrm{H^+}\, v_b\,]$ because of assumption of the same rate in Eqs. (2) and (3), for simplicity. As for the impurity current in Eq. (10), the oxidation reaction of negative ions is assumed to take place for compensation around the gold electrode, although they are not presented explicitly in the equations. Under these circumstances, the half-cell model is applied to the analysis.

5.1 Free energy of activation Δ

The activation energy is obtained by the experimental data[12]. The experiments were performed at various temperatures and the data are listed in **Table 1**. An Arrhenius plot of current versus temperature gives Δ = 0.65 eV.

Table 1 Experimental output current as a function of temperature under environmental conditions.

Temperature T(K)	290	300	310
Stable current I(nA)	20.0	57.5	104.2

5.2 Hydrogen-ion concentration

The reaction rate of antineutrino-water interaction is given by $R_{\mathrm{H_2O}} = \rho\sigma\varphi_\nu$, where ρ is the density of water molecules, σ the cross section for the dissociative ionization and φ_ν the antielectron neutrino flux. The hydrogen ion concentration $[\mathrm{H^+}\, v_b\,]$ is set at zero at the beginning and then increase as B^0 glows in water by the immersed raw silk. The increasing rate is assumed to take a form of

$$[\mathrm{H}^{+}v_b]_{rate,inc} = R_{\mathrm{H_2O}}(1/2)\{1+\tanh((t-t_d)/t_r)\}, \tag{11}$$

Where $R_{\mathrm{H_2O}}$ indicates the reaction rate of dissociative ionization of water, i.e. the product of water-molecule number density, neutrino flux of concern and dissociative-ionization cross section. The factor on $R_{\mathrm{H_2O}}$ includes t_d and t_r which express the delay and rising times in a form of 1+tanh form respectively. The delay factor is introduced to express the solved-out time of materials from raw silk in soak, and the transient effect of diffusions of ions and oxygen gas in Eqs. (2) and (3). The hydrogen ions should disappear by the rate of *1/F* as the current *I* in Eq. (4) flows. The ion concentration is assumed to be formed uniformly in the cell of apparatus. The decreasing rate of hydrogen ion concentration is written as

$$[\mathrm{H}^{+}v_b]_{rate,dec} = -I/VF, \tag{12}$$

where *V* is the volume of working cell. The sum of Eqs. (11) and (12) determines the variation of hydrogen ion concentration in the reaction. Therefore, the current density j_{H^+} in the Butler-Volmer equation in Eq. (7) is influcened by variation of $[\mathrm{H}^{+}v_b]$ through the sum of Eqs. (11) and (12).

5.3 Oxygen gas concentration

The oxygen gas concentration relative to the saturated value in water was measured[8] by Liu et al. The relative concentration was 8% immediately after starting of experiment. It considerably decreased to almost zero value in 3 days, and started to increase and reached 12% in 17 days. This indicates that the oxygen gas was generated by certain processes. The oxygen gas may be generated from either a direct process in the antineutrino-water reaction or recombination of $\mathrm{H}^{+}v_b$ and $\mathrm{OH}^{-}v_f$ under the influence of B^0 field similarly around the gold electrode. However, we regard the recombination effect to be considered in the direct reaction as the simplest approximation. Introduction of a fraction $k_{\mathrm{O_2}}$ on $R_{\mathrm{H_2O}}$ leads to

$$[\mathrm{O}_2]_{rate,inc} = k_{\mathrm{O_2}} R_{\mathrm{H_2O}}(1/2)\{1+\tanh((t-t_d)/t_r)\}. \tag{13}$$

The oxygen gas concentration increases according to this equation, while it decreases with the reduction reaction of impurity ions in Eq. (10).

5.4 Voltage across the carbon electrode

The electric voltage between gold and carbon electrodes is expressed as *IR*, where *I* is the output current and *R* the input impedance of the voltmeter. The voltage *E* between the carbon electrode and the solution may be given by $E = IR + E_{\mathrm{AU}}$, where E_{AU} serves as the correction of *E* and is mainly the potential difference between the gold electrode and the solution. We set at $E_{\mathrm{AU}} = 0$ as the half-cell model because of assumed assistance by the weak interaction. The experiment was performed at the temperature $T = 300$K, so that $k_BT = 0.0259$ eV. The carbon plate area *A* was 7 cm^2.

6. Fitting of the experimental results

Calculations were performed for the currents in **Fig. 2**. For the environmental experiment in the lower part, the current-fitting computations were made with the constraint where the experimental

behavior of oxygen gas concentration was taken into account. The fitting with $I = I_{H^+} + I_{H_2O}$ except I_{imp} represented the gradual glow of currents after 3 days, but did not reproduce the initial current peak at all. This suggests that impurity ions were solved out from the raw silk and they produced the initial peak by consuming oxygen gas. For this reason, the fitting was made by employing $I = I_{H^+} + I_{H_2O} + I_{imp}$, and the results are drawn with a solid curve in the lower part. The calculated values are somewhat lager at 5-6 days than the experimental data. This may be ascribed the simple constant value of k_{O_2} in Eq. (13). The parameters are listed in **Table 2**. The most important parameter in the fitting is the reaction rate coefficient P_c. The phosphoric-acid fuel cells basically make use of the reaction similar to Eq. (8). Since there is the difference in catalyst and operation temperature between the fuel cells and the present apparatus, the validity of P_c is not able to be discussed directly. The values of t_d and t_r were treated as adjustable parameter for expressing initiation of beginning point of weak-interaction assistance. The ICP mass measurement of ions in solution indicated that it took a few days for ions such as Ca^{2+}, Ma^{2+} to solve out into water. In addition, transient diffusion effect should appear hydrogen and hydroxide ions and oxygen corresponding to Eqs. (2) and (3). The values of t_d and t_r are considered to include these effects.

The fitting results for the experiment under natural circumstances are drawn in the lower part of **Fig. 2**. The impurity concentration $[M^{2+}]$ was applied with a time delay of 0.81 day. The impurity current and concentrations of ions are plotted in **Fig. 3 (a)**. One can see that the initial peak around 1.5 days is ascribed to the reduction of impurity ions shown by triangular marks. The initial peak current decreases soon as the oxygen gas concentration goes to zero. According to Eq. (8), the observed current depends dominantly on the concentrations of hydrogen ions and oxygen gas. The concentration of hydrogen ion varies with increase by the dissociative ionization (Eq. (11)) and decrease by the recombination into water (Eq. (12)), while that of oxygen gas is generated with Eq. (8). Fig. 3(a) indicates that the hydrogen ion concentration gradually glow due to Eqs. (11) and (13), and that of oxygen gas also slowly increases. Subsequently, the current in Eq. (8) increases up to about 50 nA. The current I_{H_2O} by the oxidation reaction also flows in the carbon electrode as in Eq. (9). This reaction is less important in most cases except the time period around 3 days. The output current increases as the accumulation of hydrogen ion and oxygen in the apparatus as inferred from Eq. (8). Oxygen gas and hydrogen ion concentrations reach almost equilibrium value after 2-3 weeks. The comparison between the experiments and calculations suggests that the half-cell model works well for the environmental experiment.

Table 2 Parameters in the half-cell model analysis.

P_c = 1.40 x 10^{34} $cm^{13}mol^{-5}s^{-1}$	R_{H_2O} = 1.81 x 10^{-13} mol $cm^{-3}s^{-1}$	$[M^{2+}]$ = 1.98 x 10^{-9} mol cm^{-3}
P_a = 1 x 10^{-3} $cm^4mol^{-2}s^{-1}$	k_{O_2} = 0.12	T_d = 2.50 d
P_i = 1.87 x 10^{27} $cm^7mol^{-3}s^{-1}$	$[O_2]_{ini}$ = 1.89 x 10^{-9} mol cm^{-3}	T_r = 1.40 d

The same parameters in **Table 2** may be applicable to the reactor-neutrino irradiation experiment, by correcting antineutrino flux by a factor of 9.5 x 10^3 during the first 3 days. However, the calculation produced the output current twice as large as the experimental data of 90 nA at a few days. The experimental current there seems to be saturated for a certain reason. A limited value was set at 9.27 x 10^{-7} mol cm^{-3} for the hydrogen concentration $[H^+ v_b]$, and it was useful to reproduce the current saturation at a few days. Nevertheless, subsequently the current slowly decreased down to 80 nA at 30 days. However, the output current was steeply reduced during the transportation to

Kyushu University and later kept to a low value. This suggests that the vibration of the apparatus during the movement may lower the concentration of ions and oxygen in the reaction cell. For this reason, the concentration of ions and oxygen were adjustably reduced to fit the experimental value during the transportation period. The calculation results are drawn in the upper part of **Fig. 2**. They fit the experimental data as a whole, but the variation around 10 days are failed to be reproduced. The value E_{AU} may deviates from zero, but it was not considered in this study.

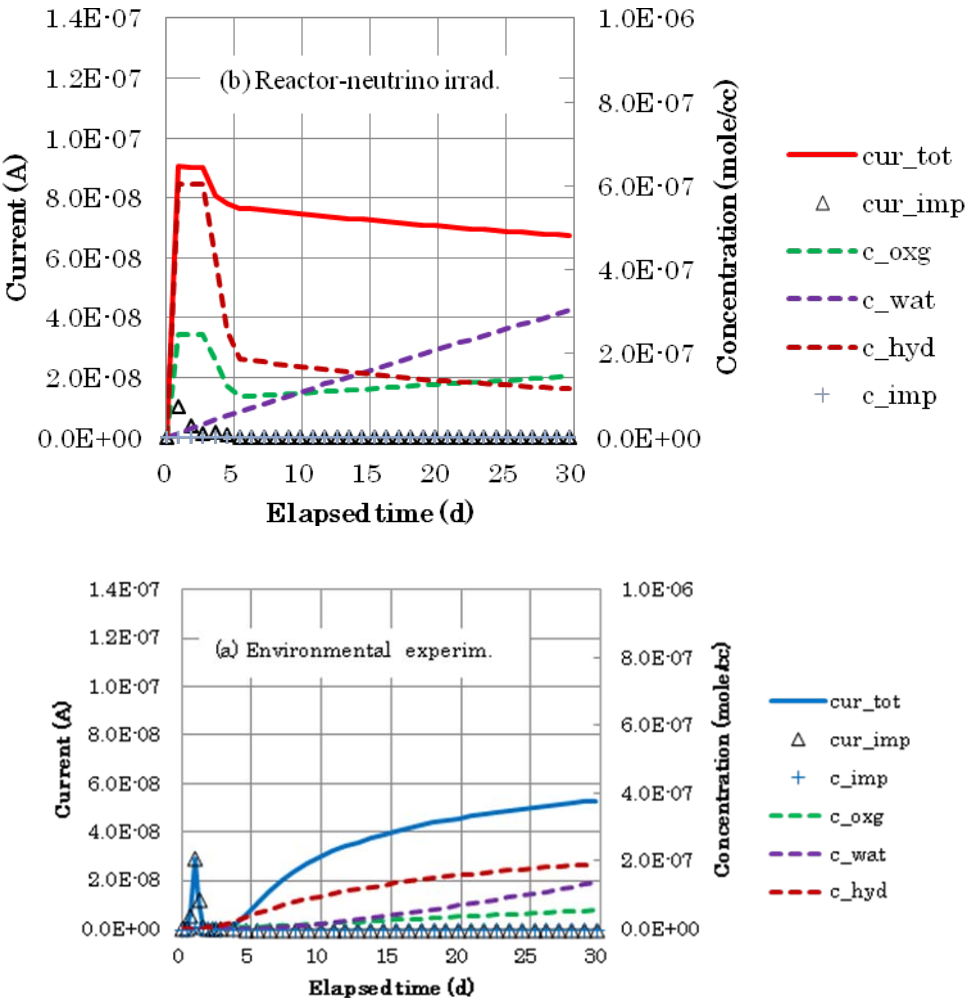

Fig. 3 Detailed results of currents and concentrations. (a) Environmental experiment at Kyushu University. (b) Reactor-neutrino irradiation and subsequent measurement.

The impurity current and the concentrations of ions are shown in **Fig. 3 (b)**. Oxygen gas and hydrogen ion concentrations reach the saturation at the first day of the experiment. They decreased quickly after stoppage of irradiation, by the influence of vibration effect of water during the transportation to Kyushu University. After the transportation, the hydrogen ion concentration is kept still high and decreases dominantly according to Eq. (12) by the excess recombination to water, while the oxygen gas concentration almost reaches the saturated value. Therefore, the current gradually decreases with elapsed time at Kyushu University.

The reaction rate of water dissociative ionization was R_{H_2O} =1.81 x 10^{-13} mol $cm^{-3}s^{-1}$. The geoneutrino flux is φ_v = 5.7 x 10^5 cm^{-2} s^{-1} in the energy region below 50 keV. The cross section of water dissociation reaction by antineutrino is estimated to be $\sigma \approx 10^{-18}$ cm^2. This value is quite large in comparison with a typical cross section around $\sigma \approx 10^{-40}$ cm^2. We consider that the compounds $H^+ v_b$ and ev_f are formed under the influence of B^0 and both have dimensions similar to an atomic size. The low energy antielectron neutrino with constituents of weak charge and weak dipole moment is estimated[6] to be in a sparse situation and be in an atomic size. A bound system in the atomic size is considered to have a binding energy comparable to energy of eV, according to a harmonic oscillator model. We can tell that a simple Born approximation for Eq. (1) with eV-range interaction energy and atomic size produces the interaction cross section of 10^{-19} cm^2. This quantity is qualitatively in agreement with the cross section from the half-cell model.

7. Conclusion

We followed the signal generation scenario that was previously proposed for the electrochemical apparatus for neutrino detection. We numerically calculated the output current in the electrochemical experiments for natural-environmental and nuclear-reactor-neutrino-irradiated conditions. The analysis was carried out with basically the same electrochemical parameters for two experiments. The weak-interaction effect on the electrochemical process included assumptions such as the bound states between neutrino fragments and dissociative-ionization products of water molecule, and the promotion of oxidation reaction around the gold electrode. Under these assumptions, the numerical analysis on the output currents lead to an admissive reproduction of two experiments. This suggests that the current generation should be ascribed to the electrochemical reaction with assist by weak interaction.

8. Acknowledgement

The authors express their gratitude to the staff of the laboratory of radiation physics and measurement for pioneering experimental data.

9. References

1) C. Quigg, “Gauge Theories of the Strong, Weak and Electroweak Interactions,” (Boulder, CO:Westview, 1998), D.H. Perkins, “Introductions to High Energy Physics,” (Menlo Park, CA: Addison-Wesley, 1988).
2) J.N. Abdurashitov, et al., *Phys. Rev. C* **60** 558011-5580132 (1999).
3) G. Kallen, *Quantum Electrodynnamics*, Springer-Verlag, Berlin (1972).
4) N. Nakanishi, *Prog.Theor.Phys.* **35**, 1111 (1967); *Prog. Theor. Phys.* **38**, 881 (1968).
5) B. Lautrup, K. Dan. *Vidensk.Selck.Mat.-Pys.Medd.* **35**, 11 (1968).
6) K. Ishibashi, N. Terao, et al., *Prog. Nucl. Sci. Technol.*, **1**, p.348-351 (2011).
7) Liu Wei, K. Ishibashi, et al., *J. Nucl. Sci. Technol., Suppl.*, **4**, 487-490 (2004).
8) K. Ishibashi, Liu Wei, et al., *Prog. Nucl. Sci. Technol.*, **1**, p.436-439 (2011).
9) T. Nishimura, Study on Neutrino Flux from Nuclear Reactor and Neutrino Structure, Doctoral dissertation, Kyushu University (2008), [in Japanese].
10) S. Enomoto, http://www.awa.tohoku.ac.jp/~sanshiro/research/geoneutrino/spectrum/index.html.

11) A.J. Bard, L.R. Faulkner, Electrochemical methods, Fundamentals and Applications, John Wiley & Sons, New York (2001).
12) Liu Wei, Study on Detection of Environmental Neutrinos by Means of Miniaturized Apparatuse Based on Electrochemical Reaction, Doctoral dissertation, Kyushu University (2004).
13) J.H. Hirschenhofer, D.B. Stauffer, et al., *Fuel Cell Handb*ook, Parsons Corp., Reading PA (1998).